

On the Use of Stochastic Resonance in Mechanical Fault Signal Detection

X.F. Zhang, N.Q. Hu, L. Zhang, X.F. Wu, L. Hu and Z. Cheng

Abstract This chapter focuses on the application of stochastic resonance (SR) in mechanical fault signal detection. SR is a nonlinear effect that is now widely used in weak signal detection under heavy noise circumstances. In order to extract characteristic fault signal of the dynamic mechanical components, SR normalized scale transform is presented and a circuit module is designed based on parameter-tuning bistable SR. Weak signal detection based on stochastic resonance (SR) can hardly succeed when noise intensity exceeds the optimal value of SR. Therefore, a signal detection model based on combination effect of colored noise SR and parallel bistable SR array, which is called multi-scale bistable stochastic resonance array, has been constructed. Based on the enhancement effect of the constructed model and the normalized scale transformation, weak signal detection method has been proposed. The effectiveness of these methods are confirmed and replicated by numerical simulations. Applications of bearing fault diagnosis show the enhanced detecting effects of the proposed methods.

1 Introduction

Weak signal detection under heavy background noise is one of the focuses in various signal-processing fields. It is commonly concerned by scientists and engineers to detect or enhance weak target signal more expeditiously and precisely in noisy environment with certain restrictions. In the real-world systems, because characteristic signals of mechanical component early fault contain a little energy and are usually annoyed by heavy noise, it is a great challenge to reveal the characteristic signal. Effective characteristic signal detection approach is significant to the fault diagnosis of mechanical component, especially when the fault is in its

X.F. Zhang · N.Q. Hu (✉) · L. Zhang · X.F. Wu · L. Hu · Z. Cheng
National University of Defense Technology, Changsha, Hunan, People's Republic of China
e-mail: hnq_5744@163.com

early stage. Prognosis of critical mechanical component mandates detecting the defect signatures as early as possible, so that the corresponding maintenance can be scheduled and the possible catastrophic accident or machine breakdown can be avoided. Consequently, detection of characteristic signal has become one of the key technologies of early fault diagnosis for mechanical component.

A traditional way of weak signal detection generally focuses on suppressing the noise to improve the output signal-to-noise ratio (SNR). Compared with conventional linear methods, the methods based on stochastic resonance (SR) are promising in the conditions of short data records and heavy noise. SR is a nonlinear effect that has been widely used in weak signal detection. Since proposed by Benzi et al. [1], stochastic resonance has been developing rapidly in signal processing, detection and estimation [2–9], especially in low SNR cases. It is essentially a statistical phenomenon resulting from an effect of noise on information transfer and signal processing that is observed in both man-made and naturally existing nonlinear systems. The counterintuitive SR phenomenon is caused by cooperation of signal (deterministic force) and noise (stochastic force) in a nonlinear system. In a certain nonlinear system, noise plays a constructive role, and energy flows from noise to signal. When noise or system parameters are tuned properly, the output SNR will reach a maximum.

However, the application of SR to practical problems has been restricted by the fact that the bistable system is only sensitive to low frequency and weak periodic signals. This can be explained in a formal way by adiabatic approximation and linear response theory [2]. In order to apply SR to high frequency signal detection, several system parameter tuning or noise intensity tuning methods have been proposed to make them more adaptive, such as normalized scale transform [10, 11], re-scaling frequency SR [12], frequency-shifted and re-scaling SR [13], adaptive step-changed [14], etc. In order to apply SR methods to characteristic vibration signal detection, two methods are discussed in this chapter: (1) normalized scale transform, a complete computation method for sampled vibration signal; (2) parameter-tuning SR circuit module for analog application. Basic theory of the two methods is parameter tuning SR. Simulations are made to validate the enhancing effect of the two methods.

The equivalence between noise tuning SR and parameter tuning SR in a typical bistable system with an additive white noise has been addressed in reference [6]. Only when the input noise intensity reaches the system resonance region, the system response is capable of following the input signal so that the output SNR is enhanced to conform to the nonlinear mechanism [5, 6]. In practice, tuning noise intensity is not always feasible. The intensities of signal and noise have been fixed for the collected raw signal in a practical engineering system. Using noise tuning, parameter tuning or array SR alone may not be a suitable option when the noise intensity exceeds the SR resonance region, which is often the case for digital signal processing and weak signal detection, such as the vibration signals collected from a gearbox for fault diagnosis and health state assessment. Besides tuning noise intensity and parameter, SR based signal processing could be improved for a better performance. The first approach is the cascaded bistable system [15],

which connects two or more bistable systems in series. The second one is the coupled or uncoupled parallel bistable array [16–19]. The third one is to make use of the characteristics of colour noise [20–22].

The SR effect can be driven not only by white noise but also by the band-limited noise alone, which indicates that it is possible to realize the SR by tuning the band limited noise. In addition, the array SR theory indicates that an array of bistable dynamical subsystems constructs a meaningful collective system for further improvement of output SNR [16–19]. In order to process the noisy signal that is beyond the SR resonance region, a summing SR array model called multi-scale bistable array (MSBA) is constructed, which consists of several bistable units. This parallel bistable array model also combines normalized scale transform with inherent SR effect driven by colour noise. At first, the processed signal is decomposed into some different scale signals by wavelet transform. Each unit is subject to different scale noise, which plays the role of inner noise of the array. The scale signal containing the target signal is processed as the noisy input signal of the array. By summing the output signal from each unit, we can obtain a resultant signal of the entire array. The signal detection method based on the MSBA can obtain a better output in high frequency signal detection under heavy noise. This method is verified and confirmed by numerical simulation and a practical case for mechanical fault diagnosis.

This chapter is organized as follows. In Sect. 2, bistable SR model is presented. In Sect. 3, normalized scale transform are introduced and validated by simulation and experiment. In Sect. 4, SR circuit module based on parameter tuning is designed and validated by simulated and experimental signal. In Sect. 5, the MSBA model is constructed and the SR effect of the model is analyzed. The signal detection approach based on MSBA is proposed and numerical simulations are carried out, which is followed by experiment on enhanced detection of rolling element bearing. Finally, the conclusions are outlined in Sect. 6.

2 Bistable Stochastic Resonance Model

The study of stochastic resonance in signal processing has received considerable attention over the last decades. In the context, stochastic resonance is commonly described as an approach to increase the SNR at the output through the increase of the special noise level at input signal. The essence of the physical mechanism underlying classical SR has been described in [1, 5, 9].

Considering the motion in a bistable double-well potential of a lightly damped particle subjected to stochastic excitation and a harmonic excitation (i.e., a signal) with low frequency ω_0 . The signal is assumed to have small enough amplitude that, by itself (i.e., in the absence of the stochastic excitation), it is unable to move the particle from one well to another. We denote the characteristic rate, that is, the escape rate from a well under the combined effects of the periodic excitation and the noise, by $\alpha = 2\pi n_{\text{tot}}/T_{\text{tot}}$, where n_{tot} is the total number of exits from one well

during time T_{tot} . We consider the behavior of the system as we increase the noise while the signal amplitude and frequency are unchanged. For zero noise, $\alpha = 0$, as noted earlier. For very small noise, $\alpha < \omega_0$. As the noise increases, the ordinate of the spectral density of the output noise at the frequency ω_0 , denoted by $\Phi_n(\omega_0)$, and the characteristic rate α increases. Experimental and analytical studies show that, until $\alpha \approx \omega_0$, a cooperative effect (i.e., a synchronization-like phenomenon) occurs wherein the signal output power $\Phi_s(\omega_0)$ increases as the noise intensity increases. Remarkably, the increase of $\Phi_s(\omega_0)$ with noise is faster than that of $\Phi_n(\omega_0)$. This results in an enhancement of the SNR. The synchronization-like phenomenon plays a key role in the mechanism as described in [23].

At present, the most common studied SR system is bistable system, which can be described by the following Langevin equation

$$\dot{x} = ax - bx^3 + A \sin(\omega_0 t + \varphi_0) + \Gamma(t) \quad (1)$$

where $\Gamma(t)$ is noise term and $\langle \Gamma(t), \Gamma(0) \rangle = 2D\delta(t)$, $A \sin(\omega_0 t + \varphi_0)$ is a periodic driving signal. Generally, it is also written as the form of Duffing equation

$$\ddot{x} = -\beta\dot{x} + ax - bx^3 + A \sin(\omega_0 t + \varphi_0) + \Gamma(t) \quad (2)$$

where β is the damping coefficient.

3 Normalized Scale Transform

3.1 Basic Theory of Normalized Scale Transform

Equation (1) has two stable solutions $x_s = \pm \sqrt{a/b} = \pm c$ (stable points) and a unstable solution $x_u = 0$ (unstable point) when $A = D = 0$, here potential of Eq. (1) is given by

$$V(x) = -\frac{1}{2}ax^2 + \frac{1}{4}bx^4 \quad (3)$$

The height of potential is

$$\Delta V = V(0) - V(c) = \frac{a^2}{4b} \quad (4)$$

When adding the modulation signal, potential function is

$$V(x, t) = -\frac{1}{2}ax^2 + \frac{1}{4}bx^4 - Ax \cos \omega_0 t \quad (5)$$

For a stationary potential, and for $D \ll \Delta V$, the probability that a switching event will occur in unit time, i.e. the switching rate, is given by the Kramers formula [2]

$$r_0 = (2\pi)^{-1} [V''(0)|V''(c)]^{1/2} \exp(-\Delta V/D) \tag{6}$$

where $V''(x) \equiv d^2V/dx^2$. We now include a periodic modulation term $A \sin \omega_0 t$ on the right-hand-side of (1). This leads to a modulation of the potential (5) with time: an additional term $-Ax \cos \omega_0 t$ is now present on the right-hand-side of (5). In this case, the Kramers rate (6) becomes time-dependent:

$$r(t) \approx r(0) \exp(-Ax \sin \omega_0 t/D) \tag{7}$$

which is accurate only for $A \ll \Delta V$ and $\omega_0 \ll \{V''(\pm c)\}^{1/2}$. The latter condition is referred to as the adiabatic approximation. It ensures that the probability density corresponding to the time-modulated potential is approximately stationary (the modulation is slow enough that the instantaneous probability density can ‘adiabatically’ relax to a succession of quasi-stationary states). The slow modulation means the signal to detect is confined to a rather low frequency range and small amplitude, and theoretical analysis and deduction are also based on this hypothesis. As we all know, the characteristic frequency reflecting mechanical system state exceeds the range of limit, so how to detect the high frequency signal is of great importance in weak characteristic signal detection of mechanical system. Here we proposed a kind of transform to solve the problem.

Considering the bistable system modeled by Eq. (1), where A is amplitude of the input signal, $\omega \gg 1$ is its frequency, $\Gamma(t)$ is Gaussian white noise with the correlation $\langle \Gamma(t) \rangle = 0$; $\langle \Gamma(t), \Gamma(0) \rangle = 2D\delta(t)$, and D is the noise intensity, when a and b are positive real numbers, take the variable substitutions

$$z = x\sqrt{b/a}, \quad \tau = at \tag{8}$$

Substituting Eq. (8) into Eq. (1), we can obtain

$$a\sqrt{\frac{a}{b}} \frac{dz}{dt} = a\sqrt{\frac{a}{b}} z - a\sqrt{\frac{a}{b}} z^3 + A \cos\left(\frac{\omega_0}{a} \tau + \phi_0\right) + \Gamma\left(\frac{\tau}{a}\right) \tag{9}$$

where the noise $\Gamma(\tau/a)$ satisfies $\langle \Gamma(\tau/a)\Gamma(0) \rangle = 2Da\delta(\tau)$. Therefore

$$\Gamma\left(\frac{\tau}{a}\right) = \sqrt{2Da}\xi(\tau) \tag{10}$$

where $\langle \xi(\tau) \rangle = 0$, $\langle \xi(\tau), \xi(0) \rangle = \delta(\tau)$.

Substituting Eq. (10) into Eq. (9), then

$$a\sqrt{\frac{a}{b}}\frac{dz}{dt} = a\sqrt{\frac{a}{b}}z - a\sqrt{\frac{a}{b}}z^3 + A \cos\left(\frac{\omega_0}{a}\tau + \phi_0\right) + \sqrt{2Da}\xi(\tau) \quad (11)$$

Equation (11) can be simplified into

$$\frac{dz}{dt} = z - z^3 + \sqrt{\frac{b}{a^3}}A \cos\left(\frac{\omega_0}{a}\tau + \phi_0\right) + \sqrt{\frac{2Db}{a^2}}\xi(\tau) \quad (12)$$

Equation (12) is a normalized form and equals to Eq. (1). The frequency of the signal after the transform is $1/a$ times of which before transform. Hence, through the chosen of larger parameter a , high frequency signal can be normalized to low frequency to satisfy the request of the theory of SR.

During the numerical simulation, the variance σ^2 is used to describe the statistical property of the white noise. As the noise intensity D is influenced by sample step h , the actual value $D = \sigma^2 h/2$.

Considering the RMS of the noise is $\sigma_0 = \sqrt{2D/h}$ before transform, after the transform, the intensity of the noise changed to $2Db/a^2$. And because the sample frequency descends, the sample step becomes a times of the original sample step. Therefore, the RMS of the noise after transform is $\sigma = \sqrt{2Db/(a^2 \cdot ah)}$. The ratio of the noise RMS after the transform to which before the transform is

$$\sigma/\sigma_0 = \sqrt{b/a^3} \quad (13)$$

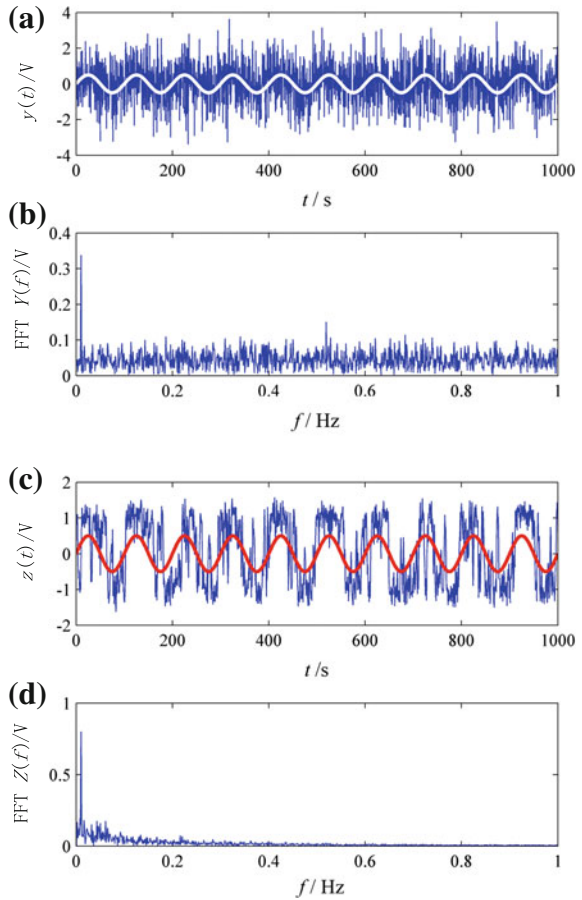
It is easy to be seen that, after the transform, the signal and noise are amplified $\sqrt{b/a^3}$ times.

3.2 Simulation Result of Normalized Scale Transform

In the following, the scale transform will be validated through a numerical simulation. We passed the mixed signal through the model of bistable system with parameters $a = b = 1$, $A = 0.3$, $f = 0.01$ Hz, $\sigma = 1.2$, and analyze the spectrum of the output signal. Figure 1a, b shows the mixed signal and its spectrum, while Fig. 1c, d gives the output of the bistable system and the spectrum of the output signal. From Fig. 1d, it can be seen that although the input SNR = $20 \log(A/\sigma) = -12.04$ dB, there is a clear spectrum line at $f = 0.01$ Hz, and the noise fades obviously.

If the signal frequency is changed to $f = 1$ kHz, according to the transform principle, we can take the parameters $a = b = 10^5$. Conditioned the mixed signal through the SR model, the result can be shown in Fig. 2. The detection result based on the normalized scale transform is shown in Fig. 2. Figure 2a, c are the

Fig. 1 Time-domain and its FFT of the input and output when $f = 0.01$ Hz. **a** and **b**: the input; **c** and **d**: the output by one-time



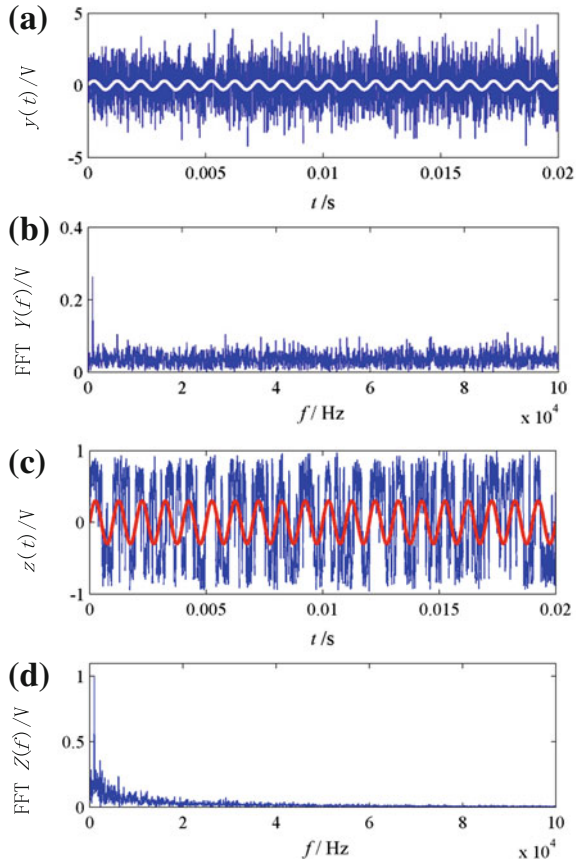
waveforms of input and output signals. Figure 2b, d are their FFT spectra. The component of 1 kHz is revealed clearly in Fig. 2d.

The signal and spectrum in Fig. 2 is consistent with Fig. 1, and the only difference is time domains and frequency coordinates of the spectrum. The noise components are greatly suppressed, and the detecting signal is standing out, which shows that the transform method is suitable to the detection of high frequency signal.

3.3 Application of Normalized Scale Transform

In cases where it is desired to process sampled discrete vibration signals, we realized that it would be possible to enhance the bearing characteristic components using SR method. As mentioned above, the SR normalized scale transform is

Fig. 2 Time-domain and its FFT of the input and output when $f = 1$ kHz. **a** and **b**: the input; **c** and **d**: the output by one-time



suitable for big parameter signal processing. In this section, SR normalized scale transform is applied in bearing fault diagnosis. The schematic diagram of bearing fault enhanced detection method is shown in Fig. 3. After sampling, the analog vibration signal is converted to input data as depicted in Fig. 3. Then, band-passed vibration signal is demodulated based on Hilbert transformation, and the output is bearing vibration envelope signal. The band-pass filter parameters are set to cover bearing natural resonance frequencies. Finally, envelope signal enhanced by SR normalized scale transform is transformed to frequency domain through FFT algorithm and fault features are extracted. The procedures of this method from input vibration data to fault features are carried out by software, in other words, achieved by computation.

This method based on SR normalized scale transform is applied to vibration signal from machinery fault simulation test rig shown in Fig. 4. Tests were carried out on the test rig with normal and planted-in inner fault bearings. The rig is driven by a variable-speed electric motor. For these tests, the shaft speed is 628 r/min with two rotor disks on the shaft. The Bearing1 in Fig. 6 is alternated with normal

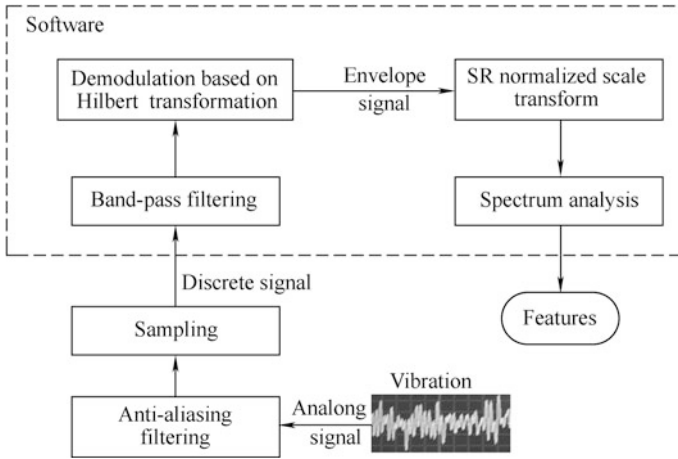


Fig. 3 Schematic diagram of enhanced bearing fault detection method using SR normalized scale transform

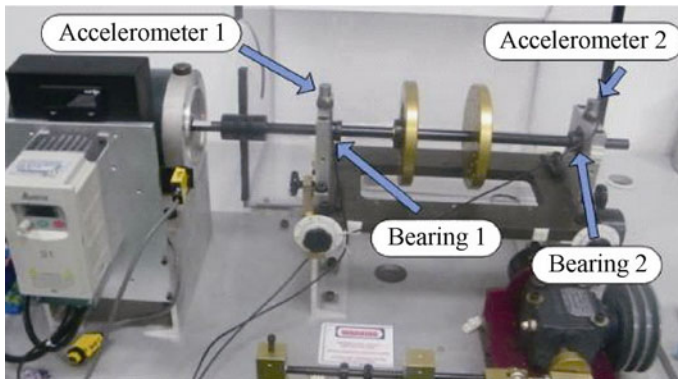


Fig. 4 Machinery fault simulation test rig

bearing, bearing with 0.2 mm planted inner race fault and bearing with 0.5 mm planted inner race fault, which are shown in Fig. 5. Signals were measured by an accelerometer on the casing immediately above it. Details of the geometry of the bearings are shown in Table 1. The expected inner race fault frequency (Ball pass frequency, inner race, BPFI) is 70.28 Hz. The raw vibration data was collected with the sampling rate 50 kHz. And the collected data length is 1 s. Figure 6 displays the recorded raw time signals from Accelerometer1 denoted in Fig. 6: (1) normal bearing, (2) bearing with 0.2 mm inner race fault and (3) bearing with 0.5 mm inner race fault.

From the raw signal we can see that there are more impacts in the vibration signals of 0.2 and 0.5 mm inner race fault than the signal of normal bearing.

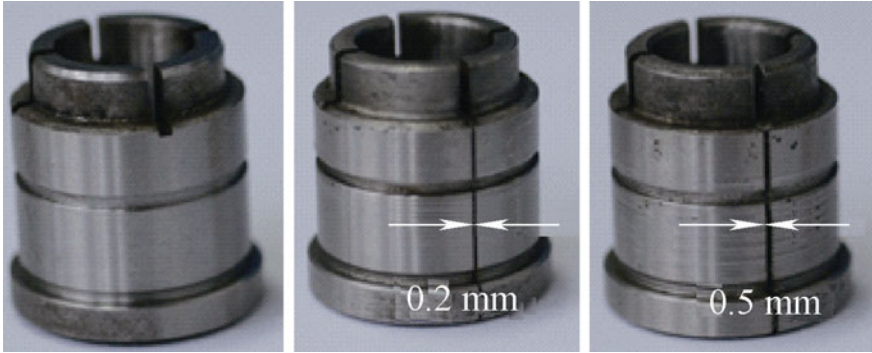


Fig. 5 Inner races of normal, with 0.2 mm planted fault and with 0.5 mm planted fault bearing (from left to right)

Table 1 Test bearing parameters

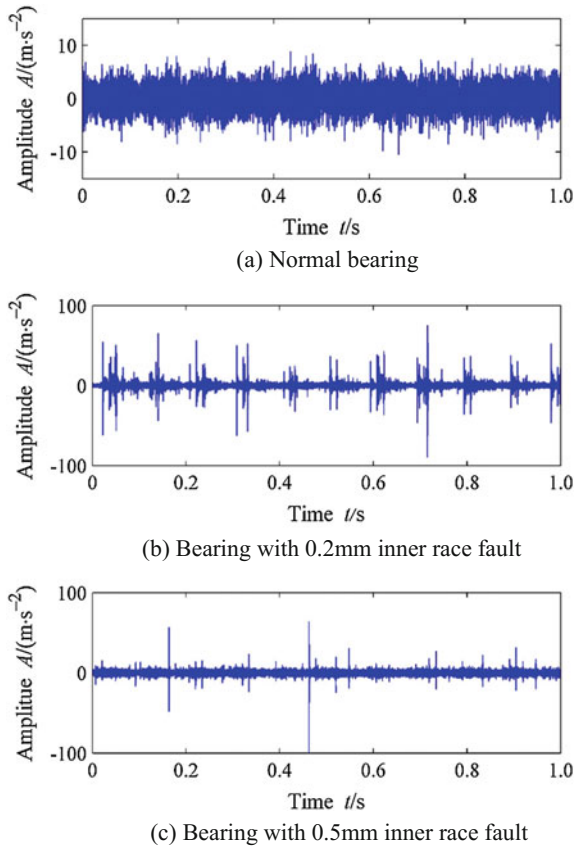
Parameter	Value
Roller diameter d /mm	7.50
Pitch diameter D /mm	34.50
Roller number n	11
Contact angle $\phi/(\text{°})$	0
Shaft speed $v/(\text{r} \cdot \text{min}^{-1})$	628

And the signal of 0.2 mm inner race fault contains obvious periodic impacts at about shaft speed, as shown in Fig. 6b. This should be caused by imbalance of the rotor system. However, we could not make sure whether there is local damage on any of the bearing component or not.

The signals were demodulated on frequency range from 8 to 12 kHz, which covers one of the bearing nature resonance bands. And Fig. 7 shows the envelope spectra of the three cases, which is up to 500 Hz—the band dominated by shaft speed, bearing fault characteristic component and their harmonics. The BPF and its harmonics are indicated by harmonic cursors in the envelope spectra. It can be seen in Fig. 7a that there are only shaft speed component and its second harmonic. In the envelope spectrum of 0.2 mm inner race fault shown in Fig. 7b, discrete spectrum components including shaft speed, BPF and their harmonics can be seen, but the BPF and the second harmonic is not clear. However, the BPF and its harmonics are obvious in Fig. 7c, since 0.5 mm inner race fault is rather severe. We use local signal to noise ratio (LSNR) as the indicator of the BPF component, which is defined as

$$R = 10 \lg \left\{ \lim_{\Delta f \rightarrow 0} \left[\int_{f-\Delta f}^{f+\Delta f} (S(f)/S_N(f)) df \right] \right\} \tag{14}$$

Fig. 6 Raw vibration signals of the experiment

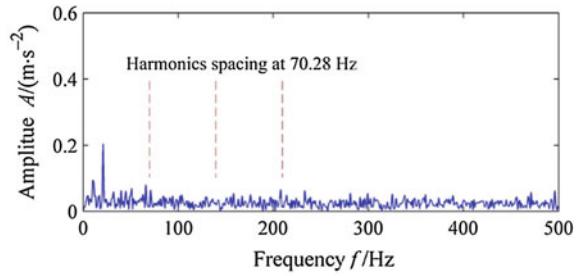


where $S(f)$ denotes the power density at signal frequency f , $S_N(f)$ is the noise mean power density around f . The LSNR indicators of envelope spectra of the three cases are 8.88, 8.58 and 14.01 dB respectively. We could not distinguish the 0.2 mm inner race fault bearing from normal bearing only by the envelope spectrum.

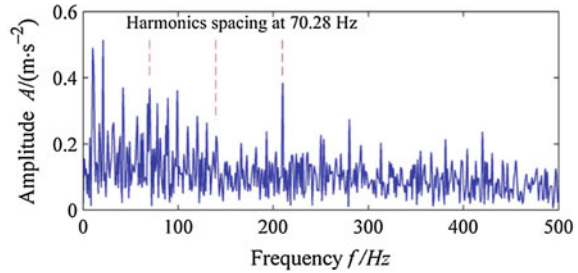
Figure 8 shows the corresponding spectra of the three signals after the vibration data are processed using the method shown in Fig. 3. The SR system parameters were tuned according to a target signal frequency of 200 Hz. It is found that the inner race fault component of 0.2 mm inner race fault was enhanced greatly, but the corresponding components of the normal bearing did not show up. The LSNR indicators of normal bearing and 0.2 mm inner fault are 8.58 and 12.22 dB. However, we could not see obvious change at the inner race fault component of the 0.5 mm inner fault case, and the LSNR indicator increases slightly to 14.16 dB. The shaft speed and its second harmonic were enhanced simultaneously in the three cases.

Although effective in the application of sampled signals processing, due to the fact that it is realized by software calculation, the normalized scale transform has

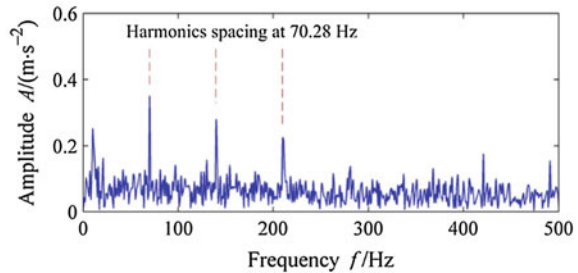
Fig. 7 Envelope spectra of the test bearings



(a) Normal bearing



(b) Bearing with 0.2mm inner race fault



(c) Bearing with 0.5mm inner race fault

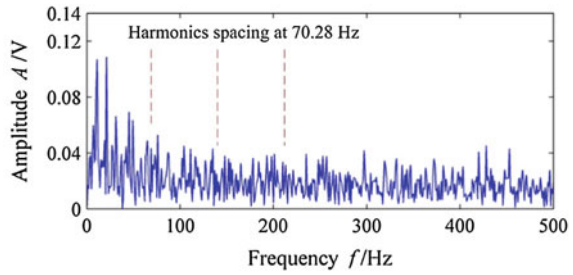
some drawbacks: (1) The sampling frequency should be much higher than the Nyquist frequency to make sure that the target signal is in the low area of whole frequency range; (2) A lot of computation is needed to obtain the solution of the differential equation.

4 SR Circuit Module

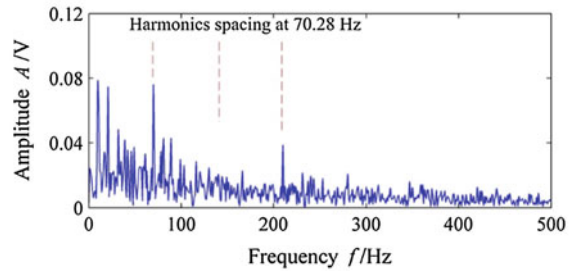
4.1 Circuit Module

Because software realization of SR requires intensive computation and high sampling frequency, it would be a practical way to actualize SR by using hardware

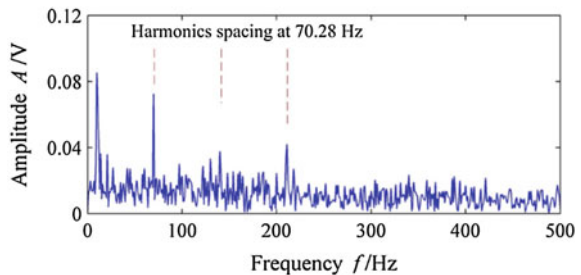
Fig. 8 Enhanced spectra of SR normalized scale transform



(a) Normal bearing



(b) Bearing with 0.2mm inner race fault



(c) Bearing with 0.5mm inner race fault

devices. To save the computational resource and the SR processing time, a circuit module is designed in this section.

The integral form of Eq. (1) is

$$x(t) = \int [ax - bx^3 + s(t) + \Gamma(t)]dt \tag{15}$$

where $s(t)$ is the signal to be detected. Equation (15) could be expressed as a nonlinear system with a feedback loop, which involves amplifier, integrator, multiplier etc. The feedback loop could be realized by amplifier, resistance and capacitances. Figure 9 is the frame and concrete SR circuit module.

According to the circuit principles, the mathematical model (nonlinear stochastic integral equation) of the circuit module can be written as

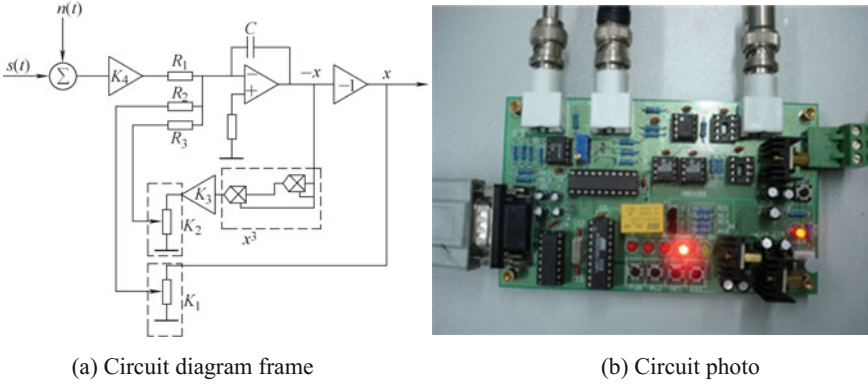


Fig. 9 Design of the SR circuit module

$$x = \int \left\{ \frac{K_4[s(t) + \Gamma(t)]}{R_1 C} - \frac{K_2 K_3 x^3}{R_3 C} + \frac{K_1 x}{R_2 C} \right\} dt \quad (16)$$

The differential form of Eq. (15) is

$$\dot{x} = \frac{K_4[s(t) + \Gamma(t)]}{R_1 C} - \frac{K_2 K_3 x^3}{R_3 C} + \frac{K_1 x}{R_2 C} \quad (17)$$

By comparing Eq. (17) and Eq. (1), the circuit system parameters can be written as $a = K_1/R_2C$, $b = K_2K_3/R_3C$, $A = K_4/R_1C$, $\Gamma'(t) = A\Gamma(t)$. The two stable status of the bistable circuit model, i.e., the two penitential wells' locations are

$$x_{1,2} = \pm \sqrt{\frac{a}{b}} = \pm \sqrt{\frac{K_1 R_3}{K_2 K_3 R_2}} \quad (18)$$

The system potential is

$$V(x) = -\frac{a}{2}x^2 + \frac{b}{2}x^4 = -\frac{1}{2} \left(\frac{K_1}{R_2 C} \right) x^2 + \frac{1}{4} \left(\frac{K_2 K_3}{R_3 C} \right) x^4 \quad (19)$$

So, the potential height is

$$\Delta V = \frac{a^4}{4b} = \frac{1}{4} \frac{K_1^2 R_3}{R_2^2 C K_2 K_3} \quad (20)$$

Equation (17) is consistent with Eq. (1) formally and intrinsically. According to bistable stochastic resonance system theory, parameter a correlates with signal frequency, and b influences ΔV . The circuit module is physically coincident with the bistable model in theory.

The parameters of the circuit R_1 , R_2 and R_3 are 10 k Ω , $C = 150$ pF, $K_3 = 0.01$. Given the other parameters, adjusting K_1 could tune a (0–666,667) to adapt to signal frequency, and adjusting K_2 could tune b (0–6667) to adapt to different noise intensity. Via adjusting resistance coefficients K_1 , K_2 or both, potential height and stable status could also be tuned. Parameters tuning can be realized by adjusting the two resistances of the circuit module designed in this section. The difference is that the input signal amplitude should be retuned based on parameters of the SR module. The weak target signal will be revealed, when signal, noise and nonlinear system are matched. Since both the input and output of circuit module are both analog signals, sampling frequency of the output signal is just demanded to catch the signal to be revealed. In other words, the high sampling frequency could be avoided. This will be validated by the simulation test in the next section.

4.2 Simulated Experiment of Circuit Module

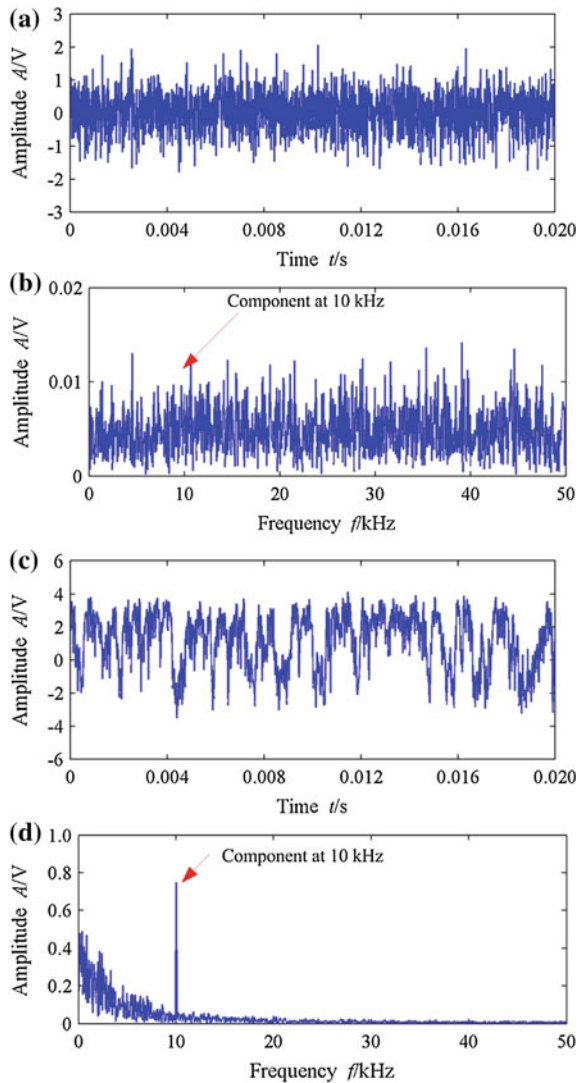
The input signal is a sinusoidal signal mixed with a white noise generated by generators. The signal frequency is 10 kHz and the amplitude is 0.04 mV. The white noise intensity RMS is 0.6 mV. Then the input signal SNR is -23.52 dB. The input signal waveform and its spectrum are shown in Fig. 10a, b.

Adjusting circuit module coefficients K_1 to 2/63 and K_2 to 50/63, that is to say, the system parameters are $a = 21,164$, $b = 5291$ and the stable states are $x_{1,2} = \pm 2$ V. The highest frequency, which could be enhanced theoretically, is calculated to 2116.4 Hz. The output signal waveform and its spectrum are shown in Fig. 10c, d. The 10 kHz signal is revealed clear in the spectrum. The signal sample frequency is 100 kHz, and the data length is 2000.

4.3 Application of Circuit Module

If SR is realized by circuit module, it would be possible to replace the SR normalized scale transform with circuit module and then change the input data to analog signal. As mentioned in Sect. 3, the sampling frequency, which could catch the signal interested under Nyquist sampling law, would be adequate for SR circuit module output signal. Moreover, there is no need to sample the signal at the beginning, if the signal processing procedures before SR circuit module are implemented by hardware. The bearing fault enhanced detection method using SR circuit module is shown schematically in Fig. 11. The parameters of SR circuit module are tuned according to the signal interested. The analog vibration signal from bearing is filtered by a band-pass filter directly. Then, the band-passed vibration signal is demodulated by envelope detection. The band-pass filter parameters are set to cover the bearing nature resonance frequency band. Envelope signal is enhanced by SR circuit module and then transformed to frequency domain

Fig. 10 Detection of 10 kHz signal by SR circuit module



through FFT algorithm after signal sampling at a much lower rate than software method. The signal processing procedures before sampling are all realized by hardware.

This method based on SR circuit module is applied to vibration signal shown in Fig. 6. Then, the analog vibration signals of the three cases were processed by hardware with SR circuit module according to the diagram shown in Fig. 11. Adjusting circuit module coefficients K_1 to $2/63$ and K_2 to $50/63$, which means that the system parameters are $a = 21,164$, $b = 5291$. The output signal of one second was collected at sampling rate 1 kHz. The FFT spectra of the three cases are shown

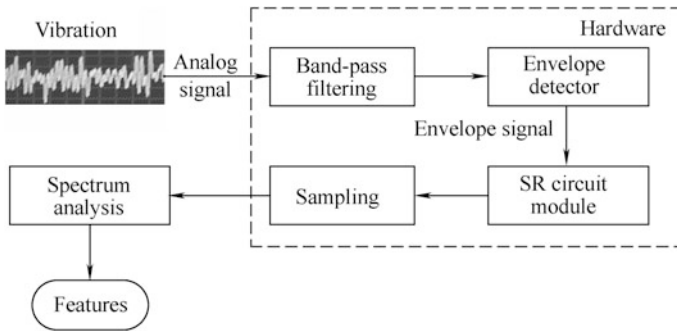


Fig. 11 Schematic diagram of enhanced bearing fault detection method using SR circuit module

in Fig. 12. Similar results to Fig. 10 were obtained with the LSNR indicators of 8.11, 12.23 and 13.67 dB. The shaft speed and its second harmonic were also enhanced simultaneously in the three cases.

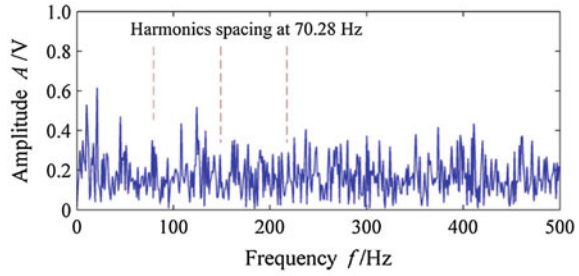
5 Multi-scale Bistable Array SR

5.1 Stochastic Resonance Effect in MSBA

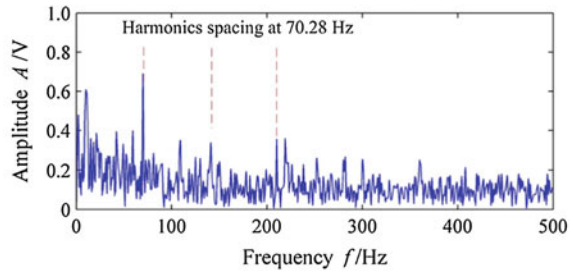
The SR effect is still shown in a nonlinear bistable system when the white noise is changed to band-limited noise, which indicates that it is possible to realize the SR by tuning the band-limited noise [5, 24]. To improve the signal processing based on SR when the original noise intensity is beyond the optimal level, the input signal is decomposed into multi-scale signals by orthogonal wavelet transform. Stationary white noise with zero mean can be decomposed into independent band-limited noises by orthogonal wavelet transform. The reconstructed detail at each scale and the approximation signal at the last scale are independent of each other owing to the orthogonality of wavelet base.

The SR effect of the bistable model of Eq. (1) is investigated using a sine signal plus a single scale noise as the input signal. By adjusting the noise intensity at each scale, Fig. 13 illustrates the SR enhancement effect of each scale noise, which indicates that SR can also be produced by each scale noise alone. The signal amplitude $A_0 = 0.3$, frequency $f_0 = 0.01$ Hz, system parameters $a = b = 1$, sampling frequency $f_s = 5$ Hz, and data length $N = 4000$. In the context, a_j and d_j denote reconstructed approximation signals and detail signals, respectively for convenience. It can be seen that the scale noise a_3 has the effect similar to the white noise, and the other scale noises still show clear SR effect when taking higher noise intensity. In a bistable system, the output SNR curves produced by different scale noises show dissimilar SR mechanisms. Now, an interesting question arises,

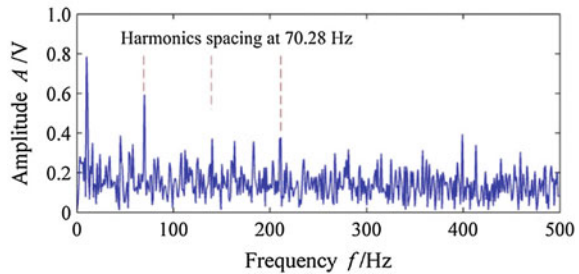
Fig. 12 Enhanced spectra of SR circuit module



(a) Normal bearing



(b) Bearing with 0.2mm inner race fault



(c) Bearing with 0.5mm inner race fault

namely, can we further improve the output SNR under large noise intensity? The answer is positive and lies in the different SR effect of each scale noise.

By combining uncoupled parallel array of dynamical subsystems with colored noise SR effect, an MSBA consisting of bistable units formulated as Eq. (1) is constructed. Figure 14 illustrates the configuration of the MSBA. The input signal is decomposed into different scale signals by wavelet transform. The driving signal of the MSBA, which is in the low frequency region, is supposed to be contained in the approximate signal a_J . The approximate signal a_J and each scale noise d_j reconstruct the new input signal of each bistable element. Then, the number of array elements is equal to the scale number J . Being uncoupled between any two elements, the outputs of all units are averaged together to produce the entire array output $y(t)$. Similar to uncoupled parallel SR array, each element is subjected to an independent array noise d_j and the same noisy input signal a_J . However, the inner

Fig. 13 Output SNR curves of SR produced by individual scale noises alone

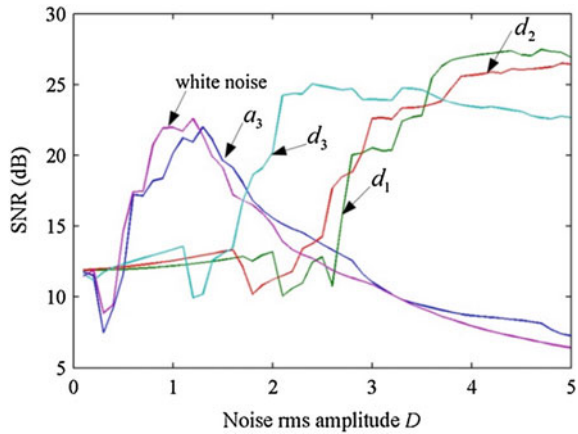
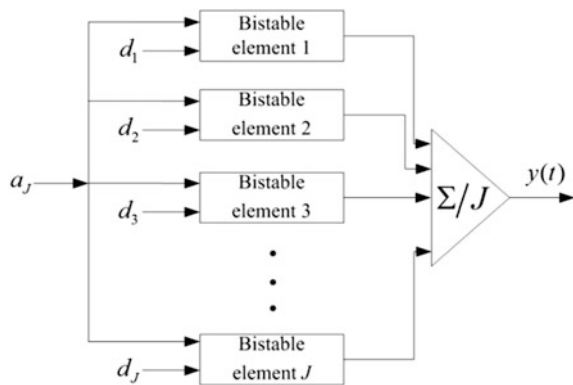


Fig. 14 MSBA model of J elements

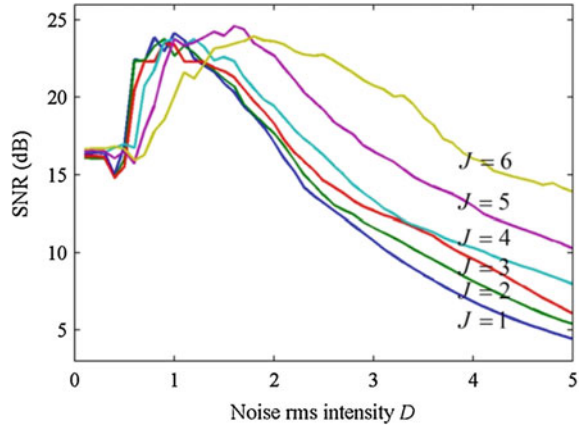


array noise intensity and characteristics of the MSBA are different from those of the uncoupled parallel array. The noise intensity of input signal is reduced after decomposition. The noise at different scale has a different contribution to the SR effect of the single bistable element in the array.

Numerical simulation is performed according to the MSBA system given in Fig. 14. Each bistable element in the MSBA is formulated as Eq. (1). The SR effect of the MSBA is evaluated with tuning the input noise intensity D and the analyzed scale number J . The other system parameters are chosen as $a = b = 1$, $A_0 = 0.3$, $f_0 = 0.01$ Hz and $\varphi = 0$. The sampling frequency is set to be $f_s = 500f_0 = 5$ Hz, and the data length of the input signal is set to be 4000.

Figure 15 shows the SR effect of the MSBA with tuning noise intensity D and the analyzed scale number J . The array output SNR curves, from bottom up, correspond to $J = 1, 2, 3, 4, 5$, and 6, respectively. The other parameters are chosen as $a = b = 1$, $A_0 = 0.3$, $f_0 = 0.01$ Hz and $\varphi = 0$. The results indicate that the tuning noise intensity D of the input signal produces an obvious SR effect on the MSBA.

Fig. 15 Output SNR of the MSBA versus tuning noise intensity D and analyzed scale number J



When the value of D increases, the array output SNR first increases and then decreases after reaching a maximum. It can be found that the output SNR resonance region is broadened with the increase of the analyzed scale number J , and also the maximum point is moved to a larger noise intensity D with almost the same value. When the noise intensity D becomes larger, the SNR curves of $J > 1$ will go up compared with the curve of $J = 1$. This means that the output signal of the MSBA has been enhanced further than that of the single bistable system at a larger input noise intensity D . Thus, the model of MSBA has admirable capability in signal processing based on SR under large noise.

The noise intensity curves of the MSBA output signal versus input noise intensity D and analyzed scale number J are shown in Fig. 16. The noise intensity curves, from top down, correspond to $J = 1, 2, 3, 4, 5$, and 6 , respectively. The other simulation parameters are the same as in Fig. 15. The output signal is filtered by a high pass filter, which is cut off at 0.1 Hz, to eliminate the driving frequency component. It can be seen that the output noise intensity is reduced gradually when the analyzed scale number J increases for a given input noise intensity. This indicates that the MSBA can achieve a better signal quality than that obtained by the conventional single SR unit.

Figure 17 compares the signal detection result of the conventional single SR unit with that of the MSBA at fixed noise intensity. The analyzed scale is $J = 6$ and the other parameters are the same as in Fig. 15. The target signal is submerged in the heavy noise ($D = 2.3$, $A_0 = 0.3$) as seen in the input signal wave in Fig. 17a. The dashed line and right y-axis in (a), (b) and (c) show the input target signal.

Comparing the output of the conventional single SR unit in Fig. 17b with that of MSBA in Fig. 17c, we can find that the MSBA can obtain smoother output waveform and lower noise. Sub-figures (d), (e) and (f) are the spectrums of sub-figures (a), (b) and (c), respectively. The above study shows that the proposed MSBA model has the capability of detecting signal under heavy noise background and can obtain the output signal with lower noise intensity correspondingly.

Fig. 16 Noise intensity curves of the MSBA output signal versus input noise intensity and analyzed scale number

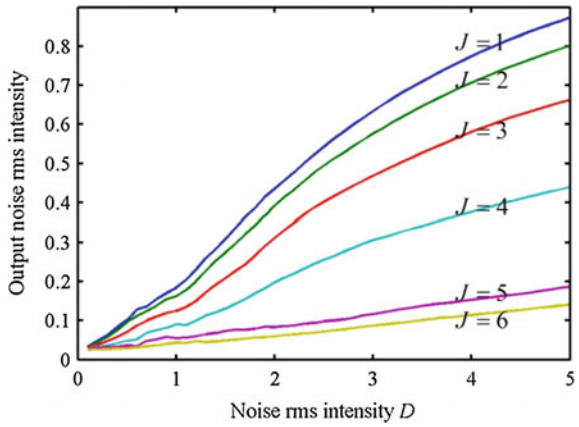
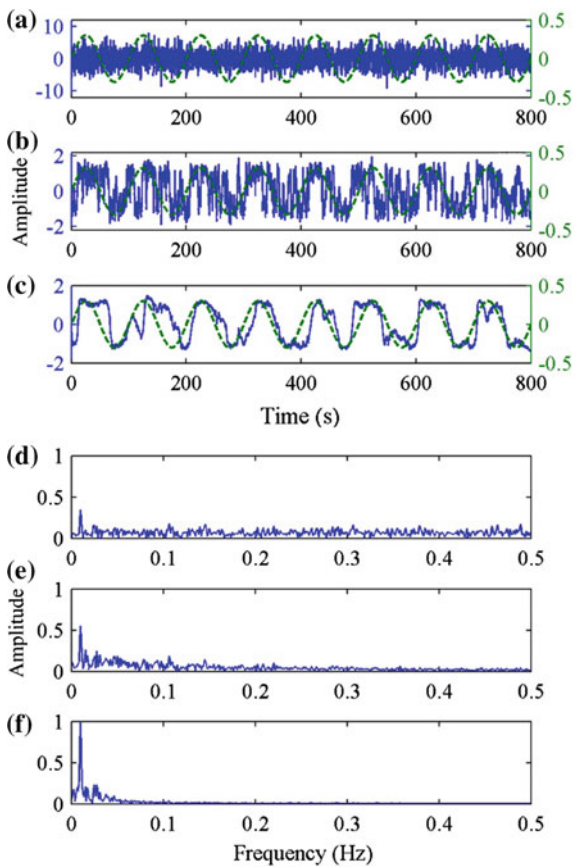


Fig. 17 Comparison of signal detection between conventional model and MSBA model



5.2 Signal Detection and Numerical Simulation

Based on the MSBA model and normalized scale transform, we present a novel weak signal detection method. The framework of the method is shown in Fig. 18. The first part is signal decomposition based on wavelet transform. a_J often contains low frequency interference which will be also enhanced by SR in practical application. The selection principle of the decomposition level J is that the d_J should cover the frequency of the target signal. Then, scale d_J is processed as the input signal of the MSBA model. The other scales of high frequency noises, as inner noises of the array, are inputted to the bistable units of MSBA, respectively. The second part is tuning MSBA parameters (a, b, k) using normalized scale transform for high frequency target signal detection, where k is the amplitude coefficient of the input signal. Finally, output signals of the units after parameter tuning are summed up and divided by the array size to obtain the resultant signal $y(t)$.

High frequency signal detection based on SR can be carried out by normalized scale transform. The SR effect of MSBA has been validated by simulation in Sect. 5.1. However, the whole enhancing effect of the combination of normalized scale transform and MSBA on weak signal still demands further verification.

Normalized scale transform consists of two parts. One is system parameter tuning for high frequency signal processing, the other is input signal amplitude tuning for output optimization. Firstly, the effect of normalized scale transform on MSBA for high frequency signal detection is illustrated by simulation. The MSBA output SNR curves of different frequency signals are depicted in Fig. 19. The tuft of six SNR curves (solid line) is corresponding to target signal frequencies $f_0 = 0.01, 0.1, 1, 10, 100$ and 1000 Hz, respectively. The sampling frequency is set to be $f_s = 500 f_0$. $a = b = f_0/0.01$, other parameters are set as the same as in Fig. 15. The effect of normalized scale transform on a single bistable unit is also shown in Fig. 19 for comparison. The tuft of six SNR curves (dashed line) is corresponding to the same target signal frequency as the MSBA model, where the parameters of the single unit are the same as the parameters of MSBA. By normalized scale transform, the target signal of different frequencies can be enhanced by SR effect in the MSBA model and the single bistable model.

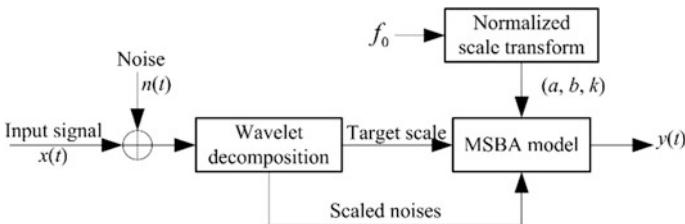


Fig. 18 Scheme of weak signal detection based on MSBA and normalized scale transform

Fig. 19 Effect of normalized scale transform on high frequency signal detection

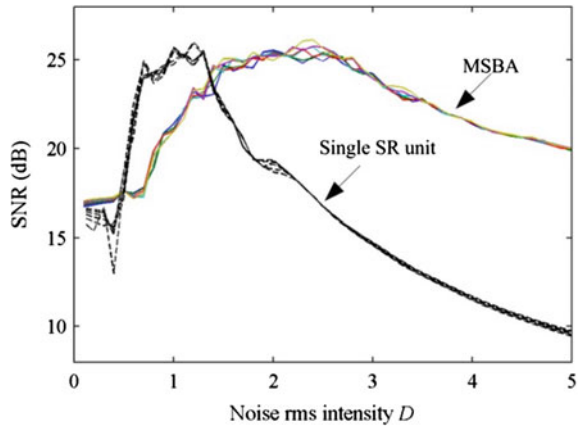
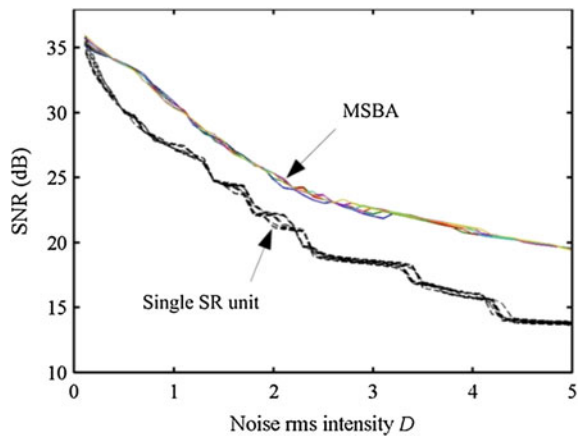


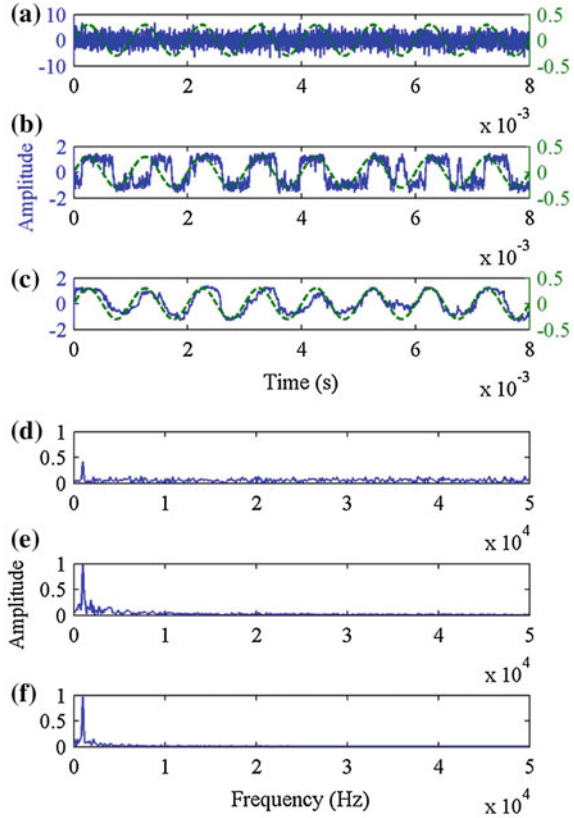
Fig. 20 SNR curves corresponding to different frequencies after amplitude tuning



Then, the effects of input signal amplitude tuning on conventional SR and MSBA are illustrated by simulation. The output SNR curves of conventional SR model (dashed line) and MSBA (solid line) after amplitude tuning are plotted in Fig. 20. The signal and system parameters used in the simulation are set to be the same as those in Fig. 19. The six curves in each tuft correspond to the target signal frequencies $f_0 = 0.01, 0.1, 1, 10, 100$ and 1000 Hz, respectively. Compared with the SNR curves in Fig. 19, the SNR curves after amplitude tuning are above the curves before amplitude tuning. Especially, the SNR is promoted greatly in the low noise intensity region.

A simulated 1 kHz target signal submerged in heavy noise ($D = 2, A_0 = 0.3$) was processed by the proposed method and the conventional SR method. The results are shown in Fig. 21. The analyzed scale is $J = 6$ and the other parameters are the same as in Fig. 15. The input signal wave is shown in Fig. 21a. The dashed

Fig. 21 Comparison of signal detection between conventional SR and the proposed method



lines and right y-axis in Figs. 21a–c show the input target signal. Comparing the output of the conventional single SR unit in Fig. 21b with that of the proposed method in Fig. 21c, we can find that the proposed method can detect the target signal explicitly and obtains an output signal with lower background noise. Figures 21d–f are the spectrums of Figs. 21a–c, respectively.

5.3 Application for Machinery Fault Diagnosis

A vibrational feature detection experiment for rolling element bearing incipient fault was conducted to verify the effectiveness of the proposed method. Bearings are widely used in mechanical transmission systems. Their local faults or damages usually produce characteristic frequency components, whose frequencies depend on bearing geometry, rotational speed and position of the fault.

Fault or defect is identified when the frequency component corresponding to the bearing defect induced impulses is found in the frequency domain. Then, the critical work is the weak characteristic signal detection after the demodulation of vibration impulses. In fact, vibration signatures in the envelope are taken to be the weak target signal and the noise and the other components are tuned to play an active role in the MSBA model. For the experiments in this section, the vibration signals are decomposed to make the scale d_J contain the characteristic frequency, where $J = 10$. In the following cases, the proposed method is verified in comparison with two other methods. One is the kurtogram for the detection of transient signal based on kurtosis maximization. The other is the conventional SR based on normalized scale transform.

The proposed method and the two other methods were applied to vibration signal from a test rig of machinery fault simulation, as shown in Fig. 22. Tests were carried out on the test rig with seeded inner and outer race fault bearings. The rig was driven by an electric motor with rotating speed 665 r/min. The vibration signals were collected with the sampling frequency of 50 kHz from the bearings with 0.2 mm seeded inner and outer race faults. The bearing with seeded defect was installed in the position of Bearing I during the test. The collected data time length was 1 s. The ball pass frequencies over inner and outer race defect, f_{BPFI} and f_{BPFO} , were computed to be 74.40 and 47.51 Hz.

Figure 23a displays the raw time signal collected from Accelerometer I on the test rig of the bearing with 0.2 mm inner race defect, which is denoted in the top right of Fig. 22. Figure 23b is the envelope of the signal in Fig. 23a processed by signal pre-whitening and signal demodulation [24]. The data in Figs. 23c, d are the output signals of the conventional SR method and the proposed method.

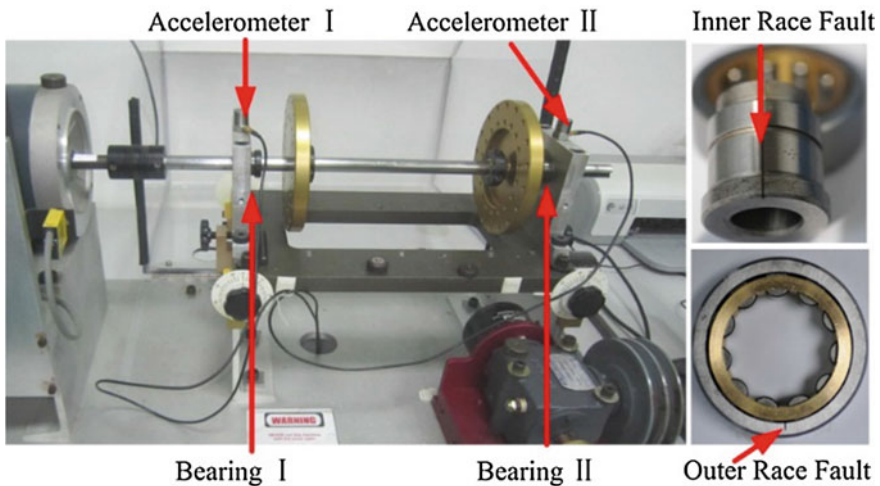


Fig. 22 Test rig and the 0.2 mm inner and outer race defect bearings

Their spectra are shown in Figs. 23e, f, respectively. It can be seen that there are some noisy impulses in the time domain signal and the envelope. The envelope signal is enhanced by traditional SR using normalized scale transform, which improves the defect identification as shown in Fig. 23e. The shaft frequency (marked as 1X) is also enhanced by the conventional SR method. The result produced by the proposed method makes the inner race fault diagnosis beyond all doubt. As seen in Fig. 23f, the characteristic component of inner race defect $f_{BPFI} = 74.40$ Hz is highlighted clearly.

Figure 24 is the analyzed result of the kurtogram, where K_{max} , B_w and f_c denote the maximum kurtosis, bandwidth and central frequency of the selected band, respectively. Figure 24a is the kurtogram of signal in Fig. 23a. Figure 24b is the envelope signal of the selected band, which maximizes the kurtogram. Figure 24c is the spectrum of the envelope signal. The characteristic component f_{BPFI} induced by inner race defect can be identified in the envelope spectrum. However, there are also some frequency components disturbing the inner race fault identification.

The vibration signal of 0.2 mm outer race fault is analyzed in Figs. 25 and 26 to confirm the reliability of the proposed method. Figure 25 displays results similar to that in Figs. 23 and 26 displays results similar to that in Fig. 24. All the signal and experimental parameters are set equal to those of the inner race fault identification. Only the fault type and the target signal frequency are different from the inner race

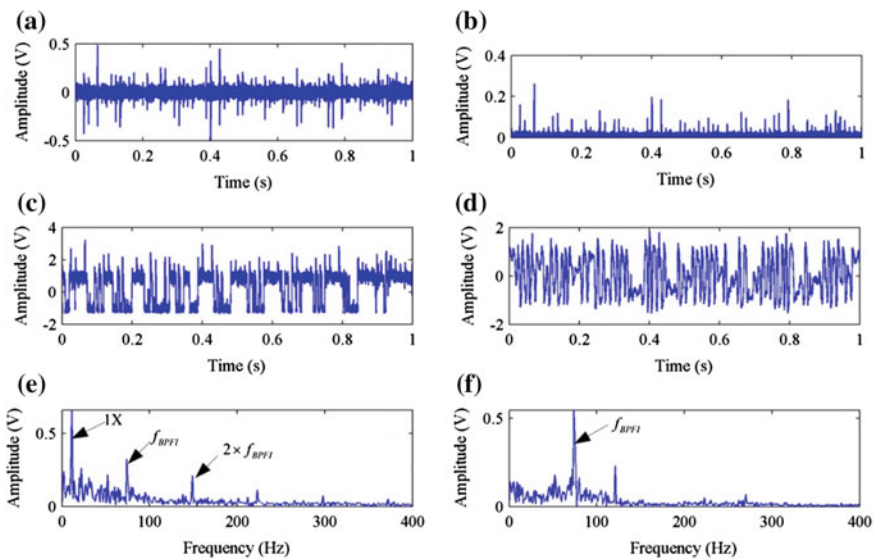


Fig. 23 Analyzed results of bearing inner race fault using the traditional SR and the proposed method

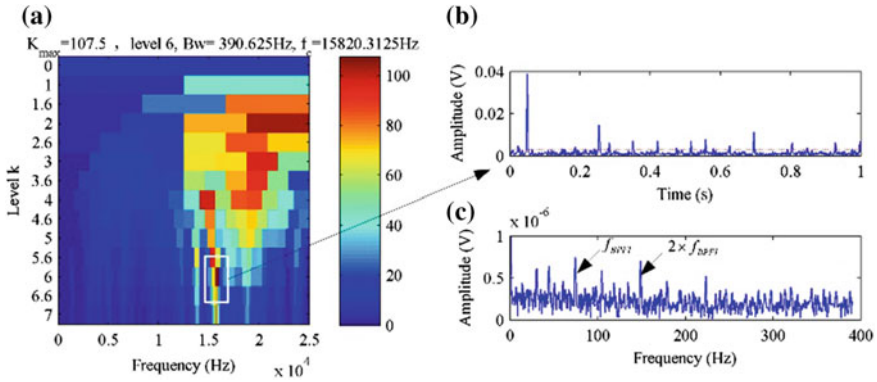


Fig. 24 Analyzed results of bearing inner race fault using kurtogram

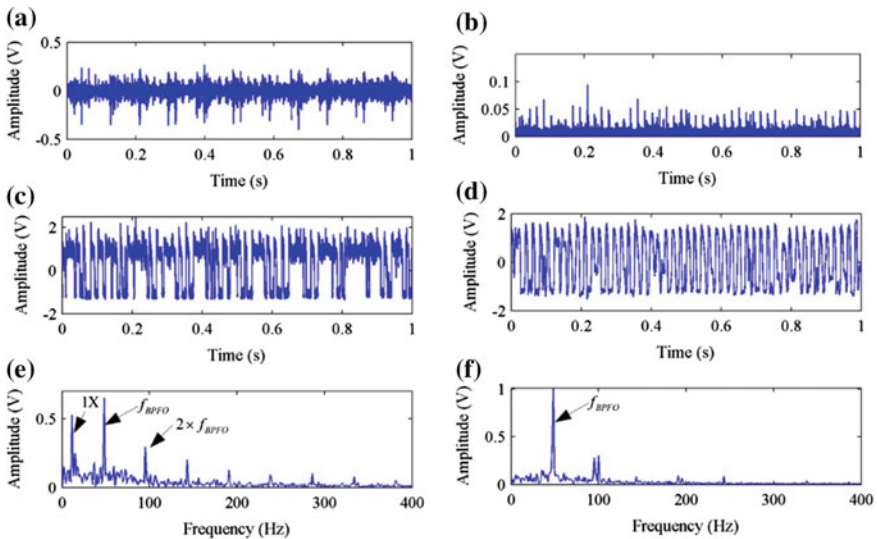


Fig. 25 Analyzed results of bearing outer race fault by using the traditional SR and the proposed method

fault identification. Similar to the result in Figs. 23 and 24, the characteristic component of outer race defect $f_{BRFO} = 47.51$ Hz is highlighted clearly by the proposed method. This shows that better performance can be achieved by the proposed method in comparison with kurtogram and traditional SR method for fault diagnosis.

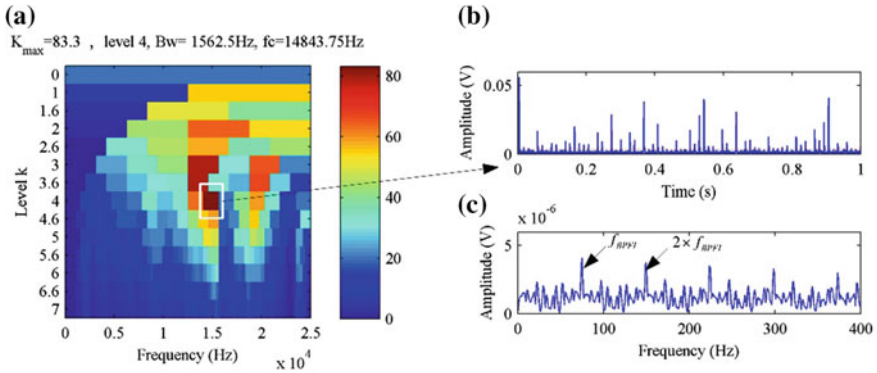


Fig. 26 Analyzed results of bearing outer race fault using kurtogram

6 Conclusions

In the chapter, we studied normalized scale transform, circuit module and multi-scale bistable array to extract characteristic fault signal of the dynamic mechanical components based on SR theory. The SR normalized scale transform is flexible and feasible for discrete signal processing, but it demands high sampling rate and expensive computation. The SR hardware module, which is suitable for processing analog signal directly, changes nonlinear system parameter tuning into resistances adjusting. The advantages of implementation by hardware are less computational task, instantaneous output, and much lower sampling frequency. The SR effect of the MSBA model could be used to detect weak signal buried by strong noise. Numerical simulation results show that the SR effect of MSBA can appear at high input noise intensity. Simulation and experiment results of the experiment on bearings with planted inner race fault demonstrate that the methods of this chapter are suitable for application in mechanical fault signal detection.

Acknowledgements The authors would like to acknowledge the support of National Natural Science Foundation of China (Grant Nos. 51475463 and 51605483) and Research Project of National University of Defense Technology (Grant No. ZK-03-14).

References

1. Benzi R., Sutera A., Vulpiana A., "The mechanism of stochastic resonance", *Journal of Physics A: Mathematical and General*, 1981, 14(11):L453–L457
2. Mcnamara B., Wiesenfeld K., "Theory of stochastic resonance", *Physical Review A*, 1989, 39(9):4854–4869
3. Jung P., Hanggi P., "Amplification of small signal via stochastic resonance", *Physical Review A*, 1991, 44(12):8032–8042
4. Bulsara A.R., Gammaitoni L., "Turning into noise", *Physics Today*, 1996, 49(3):39–45

5. Gammaitoni, L., Hanggi, P., Jung, P., et al, "Stochastic resonance", *Reviews of Modern Physics*, 1998, 70(1), 223–287
6. Xu B.H., Duan F.B., Bao R.H., et al, "Stochastic resonance with tuning system parameters: the application of bistable systems in signal processing", *Chaos, Solitons Fractals*, 2002, 13:633–644
7. Xu B.H., Li J.L., Zheng J.Y., "How to tune the system parameters to realize stochastic resonance", *Journal of Physics A: Mathematical and General*, 2003, 36(48):11969–11980
8. Xu B.H., Zeng L.Z., Li J.L., "Application of stochastic resonance in target detection in shallow-water reverberation", *Journal of Sound and Vibration*, 2007, 303:255–263
9. Hu N.Q., Chen M., Wen X.S., "The application of stochastic resonance theory for early detecting rub-impact fault of rotor system", *Mechanical Systems and Signal Processing*, 2003, 17(4):883–895
10. Yang D.X., Hu N.Q., "Detection of weak aperiodic signal based on stochastic resonance", In: 3rd International Symposium on Instrument Science and Technology, Xi'an: International Symposium on Instrument Science and Technology, 2004, 0210–0213
11. Zhang X. F., Hu N.Q., Cheng Z., et al, "Enhanced detection of rolling element bearing fault based on stochastic resonance", *Chinese Journal of Mechanical Engineering*, 2012, 25(6): 1287–1297
12. Leng Y.G., Wang T.Y., Guo Y., et al, "Engineering signal processing based on bistable stochastic resonance", *Mechanical Systems and Signal Processing*, 2007, 21:138–150
13. Tan J.Y., Chen X.F., Wang J.Y., et al, "Study of frequency-shifted and re-scaling stochastic resonance and its application to fault diagnosis", *Mechanical Systems and Signal Processing*, 2009, 23:811–822
14. Li Q., Wang T.Y., Leng Y.G., et al, "Engineering signal processing based on adaptive step-changed stochastic resonance", *Mechanical Systems and Signal Processing*, 2007, 21:2267–2279
15. Li B., Li J.M., He Z.J., "Fault feature enhancement of gearbox in combined machining center by using adaptive cascade stochastic resonance", *Sci China Tech Sci*, 2011, 54:3203–3210
16. Duan F. B., Chapeau-Blondeau F., Abbott D., "Stochastic resonance in a parallel array of nonlinear dynamical elements", *Phys Lett A*, 2008, 372:2159–2166
17. McDonnell M.D., Abbott D., Pearce C.E.M., "An analysis of noise enhanced information transmission in an array of comparators", *Microelectron J*, 2002, 33: 1079–1089
18. Stocks N.G., "Information transmission in parallel threshold arrays: suprathreshold stochastic resonance", *Phys Rev E*, 2001, 63:041114
19. Rousseau D., Chapeau-Blondeau F., "Suprathreshold stochastic resonance and signal-to-noise ratio improvement in arrays of comparators", *Phys Lett A*, 2004, 321:280–290
20. He Q.B., Wang J., "Effects of multiscale noise tuning on stochastic resonance for weak signal detection", *Digit Signal Process*, 2012, 22:614–621
21. He Q.B., Wang J., Liu Y.B., et al, "Multiscale noise tuning of stochastic resonance for enhanced fault diagnosis in rotating machines", *Mechanical Systems and Signal Processing*, 2012, 28:443–457
22. Zhang X.F., Hu N.Q., Hu L., et al, "Stochastic resonance in multi-scale bistable array", *Phys Lett A*, 2013, 377:981–984
23. Marek F., Emil S., "Stochastic resonance: a chaotic dynamics approach", *Physical Review E*, 1996, 54(2):1298–1304
24. Zhang X.F., Hu N.Q., Hu L., Zhe C., "Multi-scale bistable stochastic resonance array: A novel weak signal detection method and application in machine fault diagnosis", *SCIENCE CHINA Technological Sciences*, 2013, 56(9):2115–2123